# Prey-size plastics are invading larval fish nurseries

Jamison M. Gove[a,1,2], Jonathan L. Whitney[a,b,2], Margaret A. McManus[c], Joey Lecky[a,d], Felipe C. Carvalho[a], Jennifer M. Lynch[e,f], Jiwei Li[g], Philipp Neubauer[h], Katharine A. Smith[b,c], Jana E. Phipps[a,b], Donald R. Kobayashi[a], Karla B. Balagso[a], Emily A. Contreras[a,b], Mark E. Manuel[i,j], Mark A. Merrifield[k], Jeffrey J. Polovina[a], Gregory P. Asner[g], Jeffrey A. Maynard[l], and Gareth J. Williams[m]

[a]Pacific Islands Fisheries Science Center, National Oceanic and Atmospheric Administration, Honolulu, HI 96818; [b]Joint Institute for Marine and Atmospheric Research, University of Hawai'i at Mānoa, Honolulu, HI 96822; [c]Department of Oceanography, University of Hawai'i at Mānoa, Honolulu, HI 96822; [d]Lynker Technologies, Leesburg, VA 20175; [e]Chemical Sciences Division, National Institute of Standards and Technology, Waimanalo, HI 96795; [f]Center for Marine Debris Research, Hawai'i Pacific University, Waimanalo, HI 96795; [g]Center for Global Discovery and Conservation Science, Arizona State University, Tempe, AZ 85281; [h]Dragonfly Data Science, Te Aro, Wellington 6011, New Zealand; [i]Marine Debris Program, National Oceanic and Atmospheric Administration, Honolulu, HI 96818; [j]Freestone Environmental Services, Richland, WA 99352; [k]Center for Climate Change Impacts and Adaptation, Scripps Institution of Oceanography, La Jolla, CA 92037; [l]SymbioSeas, Carolina Beach, NC 28428; and [m]School of Ocean Sciences, Bangor University, Menai Bridge, Anglesey LL59 5AB, United Kingdom

Edited by James A. Estes, University of California, Santa Cruz, CA, and approved October 2, 2019 (received for review April 30, 2019)

**Life for many of the world's marine fish begins at the ocean surface. Ocean conditions dictate food availability and govern survivorship, yet little is known about the habitat preferences of larval fish during this highly vulnerable life-history stage. Here we show that surface slicks, a ubiquitous coastal ocean convergence feature, are important nurseries for larval fish from many ocean habitats at ecosystem scales. Slicks had higher densities of marine phytoplankton (1.7-fold), zooplankton (larval fish prey; 3.7-fold), and larval fish (8.1-fold) than nearby ambient waters across our study region in Hawai'i. Slicks contained larger, more well-developed individuals with competent swimming abilities compared to ambient waters, suggesting a physiological benefit to increased prey resources. Slicks also disproportionately accumulated prey-size plastics, resulting in a 60-fold higher ratio of plastics to larval fish prey than nearby waters. Dissections of hundreds of larval fish found that 8.6% of individuals in slicks had ingested plastics, a 2.3-fold higher occurrence than larval fish from ambient waters. Plastics were found in 7 of 8 families dissected, including swordfish (Xiphiidae), a commercially targeted species, and flying fish (Exocoetidae), a principal prey item for tuna and seabirds. Scaling up across an ∼1,000 km$^2$ coastal ecosystem in Hawai'i revealed slicks occupied only 8.3% of ocean surface habitat but contained 42.3% of all neustonic larval fish and 91.8% of all floating plastics. The ingestion of plastics by larval fish could reduce survivorship, compounding threats to fisheries productivity posed by overfishing, climate change, and habitat loss.**

larval fish | nursery habitat | surface slicks | microplastics

The majority of marine fish begin life in pelagic waters (1). Larval fish spend the first days to weeks feeding and developing at the ocean surface before recruiting to their natal habitat. Surviving this highly vulnerable life stage depends upon ocean conditions that affect food availability, growth rates, and predation (2). However, the ocean processes that influence larval fish survivorship and hence adult fish populations are poorly understood. Ocean processes that drive convergence of surface waters can form dense aggregations of planktonic organisms that represent an oasis of prey for larval fish (3). Surface slicks are narrow, meandering lines of ocean convergence that are a common feature in coastal marine ecosystems globally (4). Whether and how surface slicks are important to larval fish dynamics is currently unknown. Understanding the ocean processes that govern larval fish survivorship is critical for predicting and managing fisheries that provide sustenance and livelihood for hundreds of millions of people.

Here we show that surface slicks represent important larval fish nurseries at ecosystem scales. We studied an ∼1,000 km$^2$ area along the west coast of Hawai'i Island (hereafter West Hawai'i), the southeasternmost island in the Hawaiian Archipelago (Fig. 1*A*), where slicks are often widely distributed on the ocean surface (Fig. 1 *B* and *C*). Slicks form predominantly as a consequence of subsurface waves, called internal waves, generated by tidal flow past steep seafloor topography (4). Areas of convergence and divergence on the ocean surface form above the internal waves. The convergence areas are often rich in organic material including surfactants that modify surface tension and dampen wave-ripple formation causing a smooth, oil-slick-like appearance (5) (Fig. 2*A*). The seafloor along West Hawai'i is steeply sloped resulting in oceanic waters abutting this long coastline. Marine fish from pelagic, deep-water mesopelagic, and shallow coral reef habitats are all within a few kilometers or less of shore. We used this model system to quantify the accumulation of planktonic organisms, including larval fish, in surface slicks compared to ambient waters.

## Results and Discussion

We conducted 100 neuston (≤1-m depth) plankton tows during 3 multiday (12 to 21 d) field expeditions from 2016 to 2018 in the

### Significance

**Many of the world's marine fish spend the first days to weeks feeding and developing at the ocean surface. However, very little is known about the ocean processes that govern larval fish survivorship and hence adult fish populations that supply essential nutrients and protein to human societies. We demonstrate that surface slicks, meandering lines of convergence on the ocean surface, are important larval fish nurseries that disproportionately accumulate nonnutritious, toxin-laden prey-size plastics. Plastic pieces were found in numerous larval fish taxa at a time when nutrition is critical for survival. Surface slicks are a ubiquitous coastal ocean feature, suggesting that plastic accumulation in these larval fish nurseries could have far reaching ecological and socioeconomic impacts.**

Author contributions: J.M.G. and J.L.W. conceived the study with assistance from M. A. McManus and J.J.P.; J.L.W. led data collection and processing with assistance from J.M.G. and G.P.A.; J.M.G. and G.J.W. developed and implemented the analyses with assistance from J.L.W., J. Lecky, F.C.C., and P.N.; J. Li, K.A.S., J.E.P., D.R.K., K.A.B., E.A.C., M.E.M., and M. A. Merrifield made substantive contributions to data acquisition and materials and methods development; and J.M.G. and G.J.W. wrote the paper with assistance from J.L.W. and J.A.M.

The authors declare no competing interest.

This article is a PNAS Direct Submission.



Data deposition: All data and code used in this manuscript are in *SI Appendix* and available from NOAA's Pacific Islands Fisheries Science Center GitHub site (https://github.com/PIFSCstockassessments/fishnurseries).

[1]To whom correspondence may be addressed. Email: jamison.gove@noaa.gov.

[2]J.M.G. and J.L.W. contributed equally to this work.

This article contains supporting information online at www.pnas.org/lookup/suppl/doi:10.1073/pnas.1907496116/-/DCSupplemental.

First published November 11, 2019.

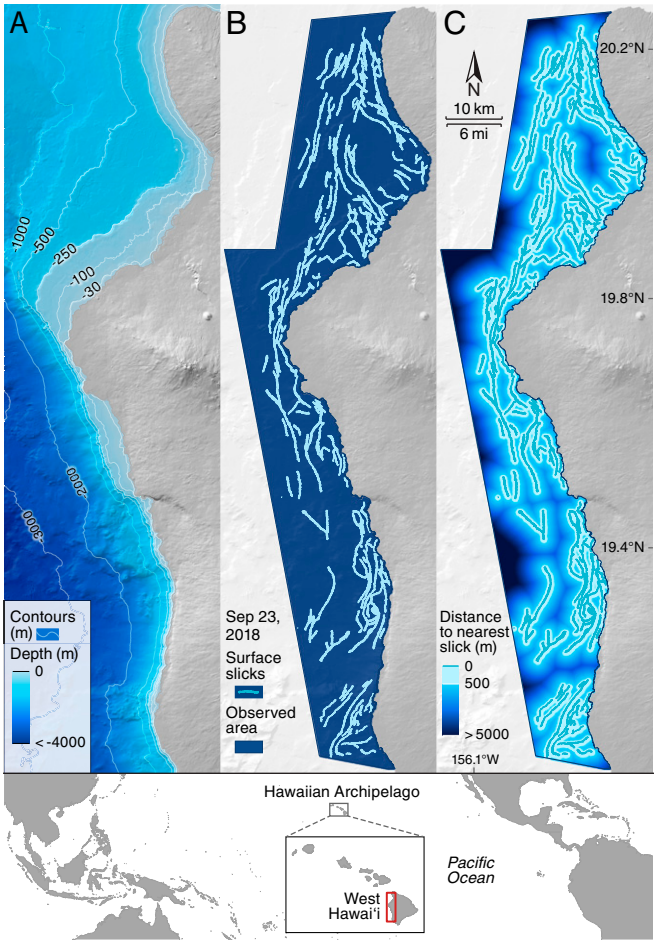


**Fig. 1.** Seafloor depths and surface slicks along the west coast of Hawai'i Island, the southeastern most island in the Hawaiian Archipelago. (*A*) Seafloor depths. (*B*) Remotely sensed observations for September 23, 2018 revealed that surface slicks and ambient waters occupied 8.8% (90 $km^2$/1,025 $km^2$) and 91.2% (935 $km^2$/1,025 $km^2$) of all nearshore (≤6.5 km) ocean surface area, respectively. (*C*) Distance to nearest slick shown in *B* with 54.0% (505 $km^2$/935 $km^2$) of all nearshore ambient waters within 500 m of a surface slick. The spatial extent of remote sensing detection is the colored region shown in *B* and *C*. For additional survey time points, the area of surface slicks and ambient waters as a percentage of the study area and the percent area of ambient waters that are within 500 m of a surface slick are as follows: August 31, 2018, 8.8% (88 $km^2$/998 $km^2$), 91.2% (910 $km^2$/998 $km^2$), and 49.2% (448 $km^2$/910 $km^2$); October 3, 2018, 9.1% (94 $km^2$/1,037 $km^2$), 90.9% (943 $km^2$/1,037 $km^2$), and 47.3% (446 $km^2$/943 $km^2$); and October 11, 2018, 6.5% (67 $km^2$/1037 $km^2$), 93.5% (970 $km^2$/1037 $km^2$), and 47.0% (456 $km^2$/970 $km^2$) (*SI Appendix*, Fig. S1).

coastal waters of West Hawai'i (*Materials and Methods*, *Neuston Tows*; *SI Appendix*, Fig. S1). We found that median densities of phytoplankton (i.e., chlorophyll-*a*), zooplankton (i.e., larval fish prey), and larval fish were 1.7-, 3.7-, and 8.1-fold higher, respectively, in surface slicks compared to neighboring ambient waters (Fig. 2*B*). The convergence of ocean surface waters aggregates marine organisms at the base of the food chain, creating complex gradients in plankton and larval fish abundance across what might otherwise appear to be a featureless ocean surface habitat.

Ocean surface productivity increases with proximity to tropical islands (6) and is further accentuated by small-scale ocean processes (7), such as surface slicks. Basal requirements for larval survival, such as food resources, are similar among fish species (8). Larval fish from multiple ocean habitats would therefore benefit from accumulated prey in surface slicks. We found the median density of larval fish from pelagic habitats, such as swordfish (Xiphiidae) and mahi-mahi (Coryphaenidae), were 28.0-fold higher in slicks over ambient waters (Fig. 2*C*). Similarly, shallow coral reef fish, including jacks (Carangidae) and goatfish (Mullidae), and deep-water mesopelagic fish, such as lanternfish (Myctophidae) and bristlemouths (Gonostomatidae), were 4.6- and 2.7-fold higher in surface slicks, respectively (Fig. 2*C*). In addition, the composition of larval fish by natal habitat differed between slicks and ambient waters. Surface slicks contained similar abundances of larval fish from pelagic (50.1%) and coral reef (44.9%) habitats (Fig. 2*D*). In contrast, ambient waters were dominated by larval coral reef fish (73.6%, Fig. 2*D*).

Development and swimming competency are important for larval fish survivorship (9). Swimming competency, including both speed and duration, increases with larval fish size and with the development of complete fin formation (1). For many tropical larval fish, fin formation occurs between 4 and 10 mm (1). We found that the median larval fish size was 6.1 mm in surface slicks ([6.2, 6.0] 95% confidence intervals [CIs]), 25.6% larger in total length than the median size of 4.8 mm found for larval fish in ambient waters ([5.0, 4.7]). The relative abundance of competent swimmers, defined here as ≥8 mm in total length, was 2.1-fold higher in surface slicks (22.7%) than in ambient waters (10.7%, Fig. 2*E*). Swimming endurance is on the order of tens of kilometers for a number of tropical larval fish (10). Based on remote sensing of surface slicks (*Materials and Methods*, *Remote Sensing*), we found that nearly half (49.4 ± 2.8%; mean ± SD) of all ambient nearshore (≤6.5 km) waters in West Hawai'i are within 500 m of a surface slick (Fig. 1*C* and *SI Appendix*, Fig. S2). This is an achievable swimming distance, particularly for larger, more well-developed larval fish. The aggregation of larger larval fish in surface slicks could result from vertical movement (i.e., swimming upward against downwelling currents), horizontal movement (i.e., directed swimming targeting slicks), or a combination of both. Given that larval fish with increased swimming competency can orient to their environment (11), tropical larval fish could be actively targeting surface slicks to capitalize on concentrated prey resources.

The fluid dynamic processes that aggregate planktonic organisms in surface slicks were also found to concentrate buoyant, passively floating plastics (Fig. 2*A*). Plastics are dispersed throughout the world's oceans (12), but are not uniformly distributed. The accumulation of plastics in large-scale oceanic features, such as subtropical gyres, has been well documented (13, 14). The degree to which plastics accumulate in local-scale (tens of meters to kilometers), ecologically important ocean surface features, such as surface slicks, was previously unknown. We found that the median plastic density was 126-fold higher in slicks than in ambient waters (Fig. 2*B*). To put this into context, median and maximum plastic densities in slicks along West Hawai'i were 8.0- and 12.7-fold higher than the respective plastic densities recently sampled in the Great Pacific Garbage Patch (13) (*Materials and Methods*, *Great Pacific Garbage Patch Comparison*). The majority of plastics sampled were small (<5 mm) fragmented pieces (*SI Appendix*, Table S2). Plastic fragments are principally derived from the breakdown of larger plastics owing to degradative processes (e.g., photodegradation, biodegradation, and hydrolysis) that can take months to years (15). While locally generated municipal waste may have contributed to the high plastic densities we observed in surface slicks off West Hawai'i, the proportion is presumed nominal given the short residence times of oceanic waters in Hawai'i and the dominance of nonlocally generated plastic pollution that accumulates on Hawai'i's beaches annually (16).

Comparing plastic with larval fish densities in slicks revealed a positive relationship ($R = 0.57$, $P < 0.001$; Fig. 3*A*), with plastics outnumbering larval fish by 7:1 (Fig. 3*B*). In contrast, the plastic-to-larval fish ratio in ambient waters was reversed (1:2) and showed no relationship ($R = 0.08$, $P = 0.62$). Along

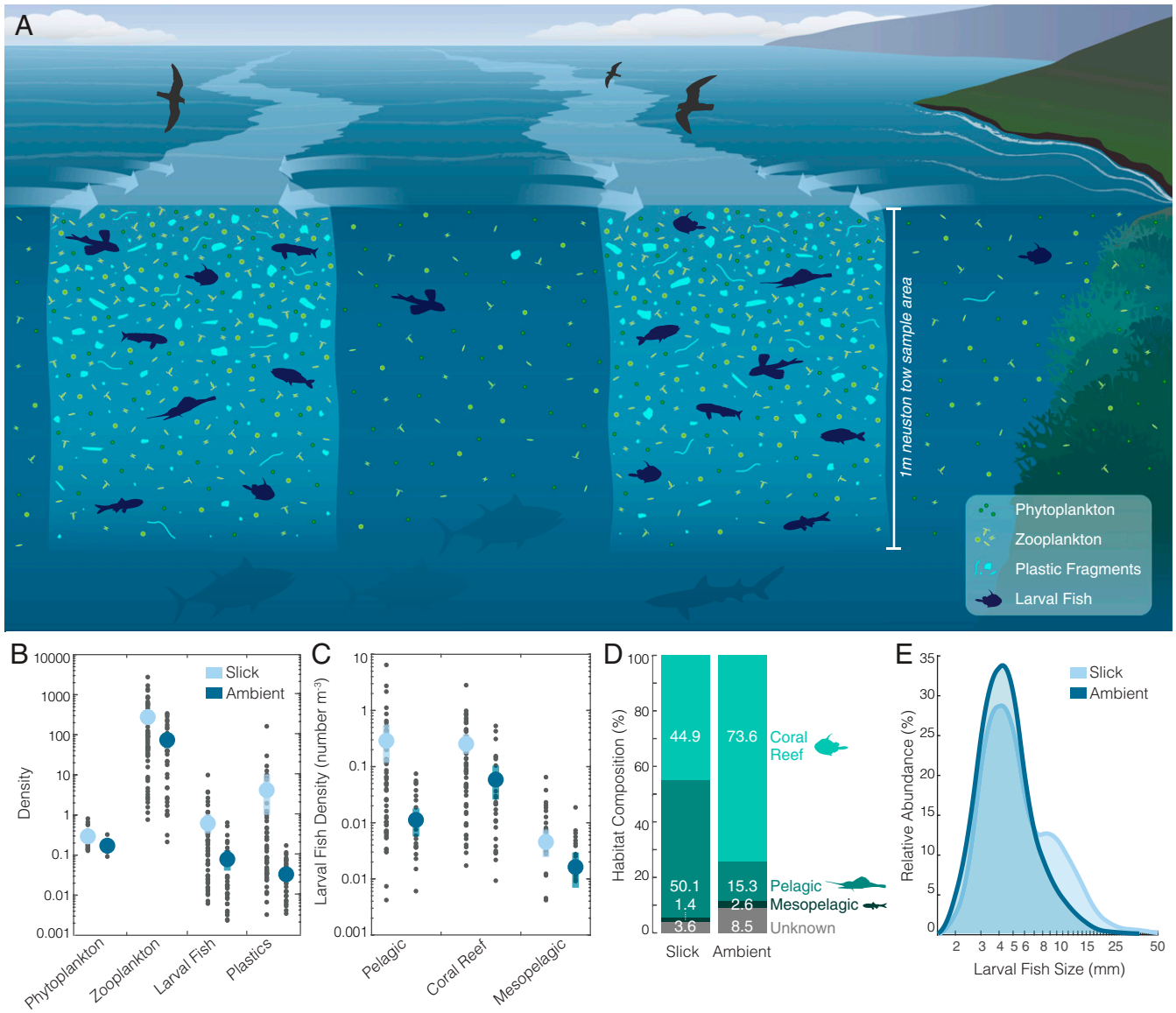


**Fig. 2.** Accumulation densities, natal habitat composition of larval fish, and larval fish size in surface slicks compared to ambient waters. (*A*) Schematic of study system with indicative slick:ambient ratios for phytoplankton, plastics, zooplankton (i.e., larval fish prey), and larval fish. Note illustrations are not to scale. (*B*) Median (upper CI, lower CI) density of phytoplankton (i.e., chlorophyll-*a*, mg $m^{-3}$), zooplankton (individuals $m^{-3}$), larval fish (individuals $m^{-3}$), and plastics (pieces $m^{-3}$). (*C*) Median density (upper CI, lower CI) of larval fish by natal habitat. (*D*) Larval fish natal habitat composition, and (*E*) relative abundance (%) of larval fish size ($n$ = 10,870 slick, $n$ = 1,032 ambient). (*B* and *C*) Gray dots indicate individual neuston tow samples as follows: chlorophyll-*a*: $n$ = 26 slick, $n$ = 9 ambient; zooplankton, larval fish, and plastics: $n$ = 63 slick, $n$ = 37 ambient. Bootstrapped median densities (95% CI) and the probability that the median density is greater in surface slicks (light blue) compared with ambient waters (dark blue) [*P*(slick)] are: chlorophyll-*a*: 0.29 [0.37,0.23], 0.17 [0.22, 0.14], P(slick) = 0.98; zooplankton: 259.91 [382.53,164.98], 69.72 [100.71,43.25], P(slick) = 0.99; larval fish: 0.60 [0.99,0.34], 0.07 [0.12,0.04], P(slick) = 1; plastic: 3.92 [9.69, 0.95], 0.03 [0.04, 0.02], P(slick) = 1; pelagic 0.33 [0.62, 0.14], 0.01 [0.02, 0.006], P(slick) = 1; coral reef: 0.25 [0.36, 0.16], 0.05 [0.10, 0.02], P(slick) = 1; mesopelagic: 0.005 [0.007, 0.003], 0.002 [0.003, 0.001], P(slick) = 0.21.

with higher densities of plastics, we found the size distribution of plastics was skewed toward smaller particles in slicks. Prey-size preference for larval fish broadly scales with their size but is generally less than 1 mm (17). The relative abundance of prey-size (≤1 mm) plastics was 40.9% higher in slicks compared to ambient waters (41.0% slicks, 29.1% ambient; Fig. 3*C*). The ratio of prey-size plastics to prey-size zooplankton was 60-fold higher in slicks (1:55) compared to ambient waters (1:3,253) (Fig. 3 *D* and *E*). Continuous fragmentation and degradation of plastics in the ocean will presumably increase the amount of prey-size plastics accumulating in surface slicks through time.

Plastics are derived from a variety of synthetic polymers (18). Polymer type dictates buoyancy characteristics, varies by product origin, and influences the toxicity potential to marine organisms (19). The composition of plastics captured in surface slicks was overwhelmingly dominated by the floating polymers polyethylene and polypropylene (97.2%; Fig. 3*F*; *Materials and Methods*, *Polymer Identification*; *SI Appendix*, Table S2). These polymers are used in single-use consumer items (e.g., plastic bags, food cartons, and bottled water) (18) and in materials commonly used in marine-based industries, such as shipping, aquaculture, and fishing (e.g., crates, buckets, rope, and nets) (20). The most dominant polymer found in slicks, polyethylene (76.6%), is known to sorb

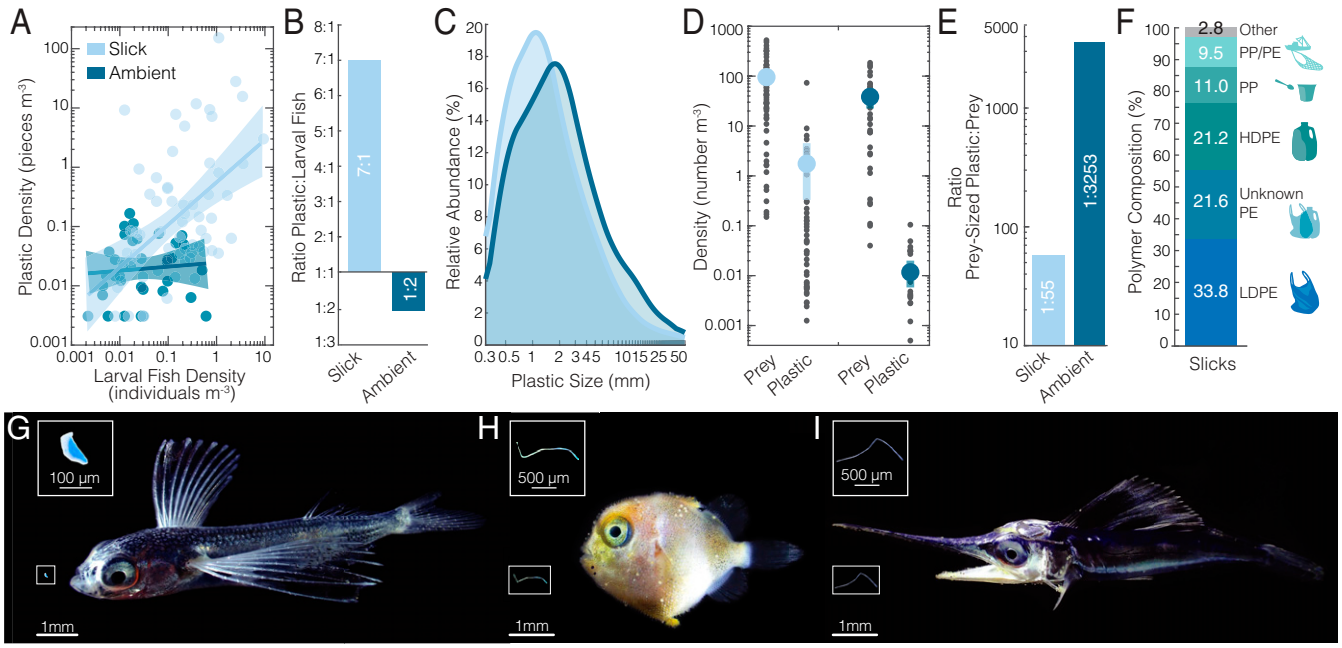


**Fig. 3.** Associations between larval fish and plastic, including prey size, in surface slicks compared to ambient waters and examples of larval fish plastic ingestion. (*A*) Linear fit (solid line) and 95% confidence intervals (CI, shaded region) of plastic (pieces $m^{-3}$) and larval fish (individuals $m^{-3}$) densities (dots) in surface slicks ($n$ = 63) and ambient waters ($n$ = 37). (*B*) Ratio of the median density of plastic to larval fish shown in Fig. 2*B*. (*C*) Relative abundance (%) of plastics by size in surface slicks ($n$ = 107,656) and ambient waters ($n$ = 480). (*D*) Median (upper CI, lower CI) densities of prey-size (≤1 mm) zooplankton (i.e., prey) and prey-size plastics ($n$ = 60 slick, $n$ = 33 ambient). Neuston plankton tow densities (grey dots) are overlaid with bootstrapped median densities (95% CI) as follows: surface slicks (light blue): prey-size zooplankton, 95.62 [129.51, 65.72] and prey-size plastic, 1.75 [4.49, 0.33]; ambient waters (dark blue): prey-size zooplankton, 39.52 [58.98, 23.66] and prey-size plastic, 0.012 [0.021, 0.006]. (*E*) Ratio of the median density of prey-size plastic to zooplankton prey shown in *D*. (*F*) Polymer composition of plastics sampled in surface slicks ($n$ = 707 pieces) as follows: LDPE, low-density polyethylene; unknown PE, unknown polyethylene; HDPE, high-density polyethylene; PP, polypropylene; PP/PE, polypropylene/polyethylene mixture. (*G–I*) Flying fish (Exocoetidae; *G*), trigger fish (Balistidae; *H*), and a billfish (Istiophoridae; *I*) collected in surface slicks with example pieces of ingested plastics.

pollutants more readily than other polymers and may serve as a vector for contaminants to marine fauna (21).

Plastic ingestion occurs in a variety of marine organisms (12), yet limited information exists for larval fish (22). To our knowledge, no prior information exists on larval fish plastic ingestion in tropical marine ecosystems. After dissecting 658 larval fish (*Materials and Methods*, *Dissections*), plastic particles were found in 42 individuals across 7 of the 8 families inspected (*SI Appendix*, Table S3). Plastic ingestion by larval fish was 2.3-fold higher ($P < 0.001$) in surface slicks (8.6%) than in ambient waters (3.7%). Plastic particles were found in commercially targeted pelagic species, including swordfish (Xiphiidae) and mahi-mahi (Coryphaenidae), as well as in coral reef species, including triggerfish (Balistidae) and sergeant majors (Pomacentridae). Plastics were also found in flying fish (Exocoetidae), a principal prey item for apex predators such as tuna (23) and most Hawaiian seabird species (24). Ingested pieces were nearly all (93%) microfibers (e.g., polyester, nylon, polyethylene terephthalate, rayon, and artificial cellulose) and were primarily blue or translucent in color (Fig. 3 *G–I* and *SI Appendix*, Table S3). Blue pigmentation is an adaptation for living at the ocean surface that is common among neustonic zooplankton (25). It is possible that larval fish confuse the thread-like ocean colored plastic particles for copepod antennae, an important prey resource (26).

Surface slicks concentrate prey-size plastics and increase the probability of encounter and ingestion by larval fish. Currently, no research exists on the physiological impacts of plastic ingestion to larval fish in the ocean. Lab-based studies are limited but reveal plastic ingestion can have adverse effects on fish, including toxicant accumulation (21), gut blockage and perforation (27), malnutrition (28), and decreased predator avoidance (29). Underdeveloped organs may hinder the ability of larval fish to detoxify and eliminate chemical pollutants (30). Therefore, the impacts of plastic ingestion to larval fish are likely more severe than to adult fish.

To assess the ecological relevance of surface slicks as nurseries at the ecosystem scale, we combined our in situ surveys with remote sensing of surface slicks across our ∼1,000 $km^2$ study region in West Hawai'i. Slicks occupied 8.3 ± 1.1% (mean ± SD) of all nearshore (≤6.5 km) ocean surface habitat but contained 42.3 ± 3.6% and 91.8 ± 1.2% of all neustonic larval fish and floating plastics, respectively (*Materials and Methods*, *Scaling up*; Fig. 1 and *SI Appendix*, Fig. S2). While most larval fish are distributed throughout the upper 100 m (31), slicks clearly provide important nursery habitat for neustonic larval fish from pelagic, mesopelagic, and coral reef habitats at ecosystem scales. Slicks provide concentrated prey resources to fish during their most vulnerable life stage. However, slicks also disproportionately accumulate nonnutritious prey-size plastics when nutrition is critical for larval fish survival. Importantly, the opportunity to directly curb larval fish exposure to plastics is tractable. Global investments that target waste management practices and consumer use would reduce the annual input of plastic to the ocean by an estimated 80% (32).

Larval fish are foundational to marine ecosystem functioning and ecosystem service provision. They are key prey for marine and terrestrial higher trophic levels (23, 24) and represent the future cohorts of the adult fish that supply protein and essential nutrients to human societies globally. Surface slicks are a ubiquitous coastal feature (4), suggesting that plastic accumulation in these larval fish nurseries could have far-reaching ecological and socioeconomic impacts. Plastic ingestion by larval fish in slicks could represent a focal point for the bioaccumulation of toxins and synthetic material across marine and terrestrial food webs. Plastic ingestion could also reduce larval fish survivorship,

compounding threats to fisheries productivity posed by overfishing, climate change, and habitat loss.

## Materials and Methods

**Study Site.** Hawai'i Island (19.55°N, 155.66°W) is the southeasternmost island of the Hawaiian Archipelago, located in the northern central Pacific (Fig. 1). The western portion, also known as West Hawai'i, has a coastline ∼315 km long and predominately oriented north to south. Wind and sea conditions are generally calm compared to most other locations in Hawai'i owing to the blocking of the northeast trade winds by 2 >4,000-m high volcanoes, Mauna Kea and Mauna Loa. The bathymetry is steeply sloped, resulting in depths of >1,000 m located within 2 km of the shoreline. Our neuston plankton sampling efforts (*Materials and Methods*, *Neuston Tows*) were conducted 0 to 6.5 km from shore (*SI Appendix*, Table S1 and Fig. S1) in an area totaling ∼1,000 $km^2$ (*Materials and Methods*, *Remote Sensing*; Fig. 1 and *SI Appendix*, Fig. S2).

**Neuston Tows.** Surface (≤1 m) planktonic organisms were sampled by towing a straight-conical ring net (1-m diameter, 4.5-m length, 335-μm mesh, 300-μm mesh soft cod ends; Sea-Gear) behind a small boat. Surface tows were conducted using a custom-built tow design sensu (33), which sampled the air–water interface to ∼1-m depth. The net was lashed to an aluminum square frame (40-mm diameter) fitted with surface displacement floats to keep the top at the air–water interface. The net was towed using an asymmetrical bridle and paravane (1.27 cm starboard) to ensure the net frame was clear of the towing vessel's wake. A mechanical flowmeter (Sea-Gear) was mounted in the mouth of the net (area = 0.79 $m^2$), providing the total volume sampled for each tow. Surface slick ($n$ = 53) and ambient water transects ($n$ = 31) were conducted for ∼8 min at a speed of ∼4 km $h^{-1}$. Transect location and length were measured using a hand-held GPS (GPSMAP78; Garmin). Tow length was 445 ± 129 m (mean ± SD, *SI Appendix*, Table S1).

In 2017, a total of 16 neuston tows were conducted from the National Oceanic and Atmospheric Administration (NOAA) ship *Oscar Elton Sette* using a 1.8-m (6 ft) Isaacs-Kidd (IK) trawl (34) equipped with a winged depressor, 505-μm mesh, and mechanical flowmeter (Sea-Gear). The IK was mounted from a J-frame crane along the midship cutout, sampled alongside to mitigate disturbance from the ship, and fished as a neuston net, sampling from slightly above the air–sea interface down to ∼1.5-m depth (mouth area = 2.75 $m^2$). Neuston tows were conducted for ∼12 min at a speed of ∼6 km $h^{-1}$. Transect location and length was measured using a hand-held GPS (GPSMAP78; Garmin). Tow length for IK neuston tows conducted from the ship was 976 ± 365 m (mean ± SD; *SI Appendix*, Table S1). NOAA scientists were stationed on the bridge to ensure the ship only sampled within a surface slick or within ambient water for the entirety of the respective transect.

Surface slicks were identified and sampled based on visual assessment. Slicks were determined by locating smooth waters with clearly identifiable edges of rippled water separated by 5 to 200 m in width and extended at least 500 m. Generally, slicks were only visible at wind speeds between 4 and 20 km $h^{-1}$. At winds <4 km $h^{-1}$ the ocean surface was predominantly smooth while at winds >20 km $h^{-1}$ the ocean surface was predominantly rippled. In each case slicks were indiscernible and therefore unable to be sampled. Transects within slicks were conducted using a sinuous tow pattern enabling the center and edges to be sampled. Plankton samples were preserved in 95% ethanol. The plankton net was cleaned between transects. Nearby ambient waters were sampled 604 ± 1,203 m (mean ± SD) away from each sampled slick. In total, we had $n$ = 63 tows from surface slicks and $n$ = 37 from ambient waters (*SI Appendix*, Table S1 and Fig. S1). Our sampling design was to pair each slick sampled with an ambient sample. However, because of inclement weather, changing wind conditions, mechanical failures, and other operational constraints, we were unable to achieve our sampling design for all slicks sampled. We ultimately had 34 samples from surface slicks that were paired with ambient waters. The mean distance from shore was 1,421 ± 1,400 m (mean ± SD) (*SI Appendix*, Table S1).

**Great Pacific Garbage Patch Comparison.** The median and maximum density of plastics from the Great Pacific Garbage Patch (GPGP) were calculated using plankton trawl data ($n$ = 500) obtained from Lebreton et al. (13). Lebreton et al. (13) neuston trawl data were downloaded from https://doi.org/10.6084/m9.figshare.5873142. Median densities were calculated from the midpoint estimates using a nonparametric bootstrap with 10,000 iterations (*Materials and Methods*, *Statistical Analyses*). Maximum values represented the respective maximum plastic density found in surface slicks and the maximum value of the higher estimate reported by Lebreton et al. (13). To ensure plastic densities from surface slicks and the GPGP were comparable, we constrained data analysis to neuston trawls conducted in the GPGP with a net mesh size of 500 μm. Further, we only included microplastics (i.e., ≤5 mm in size) in our comparison owing to the methodological approach of plastic size groupings employed by Lebreton et al. (13).

**Sample Processing.** Organisms and plastics were identified under a dissecting microscope and manually sorted into key groups: invertebrate zooplankton, fish larvae, and synthetic debris (plastics). All fish larvae were identified to the lowest taxonomic level possible, measured to total length (nearest millimeter), and counted for each sample in its entirety. Larval fish identification relied upon refs. 35–37 as sources. Invertebrate zooplankton samples were size fractioned into 3 fractions: 0.3 to 1.0 mm, 1.0 to 2.0 mm, and >2 mm, subsampled using a Folsom plankton splitter, enumerated and identified into broad taxonomic groups and life stages when possible. All counts (zooplankton, larval fish, and plastics) were standardized to the volume of water sampled for each tow and converted to densities (total number $m^{-3}$) (*SI Appendix*, Table S1).

**Dissections.** We dissected a total of 658 larval fish from 8 families, ranging in size from 5 mm to 38 mm (*SI Appendix*, Table S3). Individual fish total length was measured (to nearest millimeter) and dissected manually under stereoscopic dissecting microscopes. To minimize the risk of contamination, prior to dissections, larvae and Petri dishes were rinsed thoroughly with 70% ethanol and visually checked under the microscope to ensure no synthetic particles were adhered to larvae or dishes. Larval fish stomachs were removed, opened with microscalpels, and inspected for synthetic particles using the criteria listed above. Only particles found inside the stomach were considered (e.g., particles in the mouth were excluded). If a suspect synthetic particle was found, the particle and fish were photographed (Leica EZ4W microscope with built-in camera) and the particle was sized using ImageJ (38). To increase statistical power for slick versus ambient plastic ingestion comparisons (*Materials and Methods*, *Statistical Analyses*), larval fish sampled during the 2016 to 2018 surveys were combined with historical larval fish samples (1997 to 2011) collected via the same methodological approach (*Materials and Methods*, *Neuston Tows*) using an IK trawl aboard the NOAA ships *Townsend Cromwell* and *Oscar Elton Sette* (*SI Appendix*, Table S3). Historical data were only used for plastic ingestion comparisons. All other data analysis and information presented herein were constrained to the 2016 to 2018 surveys.

**Plastic Identification.** Plastics were manually extracted from neuston samples under dissecting microscopes and identified visually by their color, shape, and texture. We followed Norén (39) and Hidalgo-Ruz et al. (40) for visual identification of synthetic particles and used the following criteria: 1) texture should be hard, durable and not easily broken or crushed; 2) no cellular or organic structures should be visible; 3) colors should be homogenous; and 4) fibers should have uniform diameter throughout their length. Extracted plastics were dried, weighed, and photographed (Nikon D7000) under standardized lighting conditions. Images were analyzed using ImageJ (40) providing the total count, area (square millimeters) and feret diameter (i.e., maximum caliper distance) for each individual plastic particle. To reduce the possibility of counting artifacts in images (false positives), we excluded all detected particles with feret diameter <0.3 mm, which was the size of the mesh cod end for all neuston plankton tows.

**Polymer Identification.** A randomized subset (707) of particles from surface slicks was used in polymer identification (*SI Appendix*, Table S2). Each plastic piece was cleaned and analyzed using a PerkinElmer attenuated total reflectance Fourier transform infrared (ATR FT-IR) Spectrometer Spectrum Two according to Jung et al. (41). The ATR FT-IR crystal was cleaned with isopropanol and a background spectrum was run before each sample. Samples were applied to the crystal with a force between 80 and 100 N. Spectra were analyzed manually. A minimum of 4 matching absorption bands were required for polymer identification (41). A subset of particles and microfibers ingested by larval fish were selected for polymer identification using both Raman microscopy and attenuated total reflectance Fourier transform infrared microscopy (*SI Appendix*, Table S3). See *SI Appendix*, *Methods* for more details on ingested polymer identification.

**Water Samples.** We collected surface water samples at a subset of slick and ambient transects to determine concentrations of chlorophyll-*a* (*SI Appendix*, Table S1). Samples for chlorophyll-*a* were collected by hand using a 250-mL dark Nalgene bottle and immediately placed on ice while in the field. Water samples were later filtered onto 25-mm glass microfiber filters (Whatman),

placed in 10 mL of 90% acetone, frozen for 24 h, and then analyzed for chlorophyll-*a* concentration using a Turner Designs model 10AU fluorometer.

**Remote Sensing.** Planet Dove satellite images (https://www.planet.com/) were utilized due to their daily revisit frequency and high spatial resolution (3.7 m). Our mapping approach utilized the contrast between the surface texture of slicks and regular seawater, which is most significant when sun glint is observed in the satellite images (42, 43). A total of 97 cloud-free, sun-glint-saturated Dove reflectance images were selected from Planet to cover the study area. Images were selected in the following time steps in 2018 to assess surface slick spatial distribution and extent: August 31, September 23, October 3, and October 11 (Fig. 1*B* and *SI Appendix*, Fig. S2). See *SI Appendix, Methods* for further details on the identification of surface slicks from satellite imagery.

**Geospatial Analysis.** Bathymetry data (Fig. 1*A* and *SI Appendix*, Fig. S1) were obtained from the University of Hawai'i (http://www.soest.hawaii.edu/HMRG/multibeam/bathymetry.php). All geospatial analyses were performed in ArcGIS Desktop 10.6 software (http://desktop.arcgis.com) with the extensions and tools specified below. Geospatial information was derived for the surface slicks identified with Planet Dove satellite imagery (see *Materials and Methods*, *Remote Sensing*). For each time point, the geographic area (square meters) and percent area (%) of slick coverage was calculated in projected coordinate system Universal Transverse Mercator (UTM) zone 5N, World Geodetic System (WGS) 1984. We then produced a raster dataset for each time point that represented the distance to the nearest slick footprint for each pixel by using the Euclidean Distance tool (Spatial Analyst extension) at the native resolution of the Dove imagery. Distance surfaces were clipped to the study area defined by the Dove imagery mosaics (Fig. 1*C* and *SI Appendix*, Fig. S2). Summary calculations for distance to nearest slick were derived for 0 to 6.5 km from shore, which represented the furthest offshore extent of our neuston plankton sampling efforts (*Materials and Methods*, *Neuston Tows*; *SI Appendix*, Table S1 and Fig. S1).

Distance to shore for each neuston transect (*SI Appendix*, Table S1) was calculated as the shortest distance from the shoreline to the centroid of the GPS track using Near Analysis tools.

**Scaling up.** To estimate the percentage of larval fish and plastics in surface slicks across our ~1,000-km$^2$ study area, we first multiplied the ocean surface area of slicks and ambient waters for each time point (*Materials and Methods*, *Remote Sensing*) by each of the 10,000 bootstrap replicates of median larval fish and plastic densities (*Materials and Methods*, *Statistical Analyses*). We then calculated the median of these 10,000 population estimates for larval fish and plastics in slicks as a percentage of the total study area observed for each time point. All calculations were constrained to the spatial extent of our neuston plankton samples (≤6.5 km).

**Statistical Analyses.** Individual neuston tow density values were calculated by dividing the numerical abundance of each group (e.g., larval fish) by the total volume of water sampled for each tow. Nonparametric bootstrap was used in order to explicitly investigate the uncertainty (i.e., 95% confidence intervals) associated with median density values in each group. The bootstrap was based on random sampling (with replacement) from the original densities for each group separately. Nonparametric bootstrap was preferred in order to avoid explicit assumptions about the distribution of density values. The confidence intervals for median densities were based on 10,000 bootstrap replicates. The same approach was applied to fish size, except with 20,000 bootstrap replicates owing to the large sample size ($N$ = 11,902).

A permutation test was used to calculate the empirical probability that the median density (Md) of chlorophyll-*a*, zooplankton, larval fish (including pelagic, coral reef, and mesopelagic), and plastics inside ($Md_i$; "slick") is larger than median density outside ($Md_o$; "ambient waters") in our study [$P(Md_i > Md_o)$]. The empirical probability was calculated by randomly permuting the group labels (inside and outside), each time recalculating the difference between median group densities. $P(Md_i > Md_o)$ was then calculated as the proportion of replicates for which the permuted difference of medians was larger than the difference of group medians in the original data. The same analytical approach was applied to fish size.

Distribution (probability of presence) of plastic in the stomachs of fish was assessed using a generalized linear model (GLM) with a binomial distribution of error and a logit link. The GLM has a binary response ranging between 0 (absence of plastic) and 1 (presence of plastic) and tested for a significant difference (alpha = 0.05) in the presence of plastic within fish dissected from inside (i.e., slick) and outside (i.e., ambient waters) in our study.

**ACKNOWLEDGMENTS.** We thank Dieter Tracey for graphics help with Fig. 1 and *SI Appendix*, Figs. S1 and S2 and Amanda K. Dillon for graphics support on Figs. 2 and 3. We thank Daniel Jennings-Kam, Andrew Osberg, Dalton Solbrig, and Lauren Zodl for their assistance with plankton sample sorting and Bruce Mundy for his assistance with larval fish identifications. We thank Anupam Misra, Lloyd Hihara, Jan Kealoha, Kayla Brignac, Wanda Weatherford, Bridget O'Donnell, and Suja Sukumaran for their assistance with microfiber identification. We also thank the three anonymous reviewers for their insightful comments on this manuscript. Finally, we thank the crew of the NOAA ship *Oscar Elton Sette*. This research was supported by NOAA's West Hawai'i Integrated Ecosystem Assessment (contribution no. 2019_4), NOAA's Fisheries And The Environment program, and NOAA's Pacific Islands Fisheries Science Center.

1. J. M. Leis, M. I. McCormick, "The biology, behavior, and ecology of the pelagic, larval stage of coral reef fishes", in *Coral Reef Fishes: Dynamics and Diversity in a Complex Ecosystem*, P. F. Sale, Ed. (Academic Press, San Diego, CA, 2002), pp. 171–199.
2. B. H. Letcher, J. A. Rice, L. B. Crowder, K. A. Rose, Variability in survival of larval fish: Disentangling components with a generalized individual-based model. *Can. J. Fish. Aquat. Sci.* **53**, 787–801 (1996).
3. M. Kingsford, J. Choat, Influence of surface slicks on the distribution and onshore movements of small fish. *Mar. Biol.* **91**, 161–171 (1986).
4. C. B. Woodson, The fate and impact of internal waves in nearshore ecosystems. *Annu. Rev. Mar. Sci.* **10**, 421–441 (2018).
5. S. A. Ermakov, E. N. Pelinovsky, Variation of the spectrum of wind ripple on coastal waters under the action of internal waves. *Dyn. Atmos. Oceans* **8**, 95–100 (1984).
6. J. M. Gove *et al*., Near-island biological hotspots in barren ocean basins. *Nat. Commun.* **7**, 10581 (2016).
7. C. B. Woodson, S. Y. Litvin, Ocean fronts drive marine fishery production and biogeochemical cycling. *Proc. Natl. Acad. Sci. U.S.A.* **112**, 1710–1715 (2015).
8. W. Leggett, E. Deblois, Recruitment in marine fishes: Is it regulated by starvation and predation in the egg and larval stages? *Neth. J. Sea Res.* **32**, 119–134 (1994).
9. C. B. Paris, R. K. Cowen, Direct evidence of a biophysical retention mechanism for coral reef fish larvae. *Limnol. Oceanogr.* **49**, 1964–1979 (2004).
10. I. C. Stobutzki, D. R. Bellwood, Sustained swimming abilities of the late pelagic stages of coral reef fishes. *Mar. Ecol. Prog. Ser.* **149**, 35–41 (1997).
11. J. M. Leis, Are larvae of demersal fishes plankton or nekton? *Adv. Mar. Biol.* **51**, 57–141 (2006).
12. H. S. Auta, C. U. Emenike, S. H. Fauziah, Distribution and importance of microplastics in the marine environment: A review of the sources, fate, effects, and potential solutions. *Environ. Int.* **102**, 165–176 (2017).
13. L. Lebreton *et al*., Evidence that the great Pacific garbage patch is rapidly accumulating plastic. *Sci. Rep.* **8**, 4666 (2018).
14. M. Eriksen *et al*., Plastic pollution in the world's oceans: More than 5 trillion plastic pieces weighing over 250,000 tons afloat at sea. *PLoS One* **9**, e111913 (2014).
15. Y. K. Song *et al*., Combined effects of UV exposure duration and mechanical abrasion on microplastic fragmentation by polymer type. *Environ. Sci. Technol.* **51**, 4368–4376 (2017).
16. H. S. Carson *et al*., Tracking the sources and sinks of local marine debris in Hawai'i. *Mar. Environ. Res.* **84**, 76–83 (2013).
17. L. Carassou, R. Le Borgne, D. Ponton, Diet of pre-settlement larvae of coral-reef fishes: Selection of prey types and sizes. *J. Fish Biol.* **75**, 707–715 (2009).
18. PlasticsEurope, "Plastics—The facts 2016: An analysis of european plastics production, demand and waste data." https://www.plasticseurope.org/en/resources/publications/3-plastics-facts-2016. Accessed 17 October 2019.
19. C. M. Rochman, E. Hoh, B. T. Hentschel, S. Kaye, Long-term field measurement of sorption of organic contaminants to five types of plastic pellets: Implications for plastic marine debris. *Environ. Sci. Technol.* **47**, 1646–1654 (2013).
20. M. R. Jung *et al*., Polymer identification of plastic debris ingested by pelagic-phase sea turtles in the central Pacific. *Environ. Sci. Technol.* **52**, 11535–11544 (2018).
21. C. M. Rochman, E. Hoh, T. Kurobe, S. J. Teh, Ingested plastic transfers hazardous chemicals to fish and induces hepatic stress. *Sci. Rep.* **3**, 3263 (2013).
22. M. Steer, M. Cole, R. C. Thompson, P. K. Lindeque, Microplastic ingestion in fish larvae in the western english channel. *Environ. Pollut.* **226**, 250–259 (2017).
23. P. J. Rudershausen *et al*., Feeding ecology of blue marlins, dolphinfish, yellowfin tuna, and wahoos from the North Atlantic Ocean and comparisons with other oceans. *Trans. Am. Fish. Soc.* **139**, 1335–1359 (2010).
24. C. S. Harrison, T. S. Hida, M. P. Seki, Hawaiian seabird feeding ecology. *Wildl. Monogr.* **85**, 3–71 (1983).
25. P. J. Herring, Blue pigment of a surface-living oceanic copepod. *Nature* **205**, 103–104 (1965).
26. J. K. Llopiz, R. K. Cowen, Variability in the trophic role of coral reef fish larvae in the oceanic plankton. *Mar. Ecol. Prog. Ser.* **381**, 259–272 (2009).
27. E. J. Carpenter, S. J. Anderson, G. R. Harvey, H. P. Miklas, B. B. Peck, Polystyrene spherules in coastal waters. *Science* **178**, 749–750 (1972).
28. R. Gregory Murray, Environmental implications of plastic debris in marine settings—entanglement, ingestion, smothering, hangers-on, hitch-hiking and alien invasions. *Phil. Trans. Royal Soc. Biol. Sci.* **364**, 2013–2025 (2009).
29. L. Carlos de Sá, L. G. Luís, L. Guilhermino, Effects of microplastics on juveniles of the common goby (Pomatoschistus microps): Confusion with prey, reduction of the predatory performance and efficiency, and possible influence of developmental conditions. *Environ. Pollut.* **196**, 359–362 (2015).

30. A. Mohammed, "Why are early life stages of aquatirc organisms more sensitive to toxicants than adults?" in *New Insights into Toxicity and Drug Testing*, S. Gowder, Ed. (IntechOpen, Rijeka, Croatia, 2013), pp. 49–62.
31. G. W. Boehlert, W. Watson, L. C. Sun, Horizontal and vertical distributions of larval fishes around an isolated oceanic island in the tropical Pacific. *Deep-Sea Res.* **39**, 439–466 (1992).
32. J. R. Jambeck *et al*., Marine pollution. Plastic waste inputs from land into the ocean. *Science* **347**, 768–771 (2015).
33. D. Brown, L. Cheng, New net for sampling the ocean surface. *Mar. Ecol. Prog. Ser.* **5**, 224–227 (1981).
34. R. F. Devereux, R. C. Winsett, Isaacs-Kidd midwater trawl (Scripps Institution of Oceanography, 1953), SIO Reference 53-3.
35. J. M. Leis, B. M. Carson-Ewart, *The Larvae of Indo-Pacific Coastal Fishes: An Identification Guide to Marine Fish Larvae* (Brill, 2000), **vol. 2**.
36. J. M. Miller, J. M. Leis, W. Watson, *An Atlas of Common Nearshore Marine Fish Larvae of the Hawaiian Islands* (University of Hawaii Sea Grant College Program, 1979).
37. H. Moser, The early stages of fishes in the California current region. *Calcofi Atlas* **33**, 1505 (1996).
38. C. A. Schneider, W. S. Rasband, K. W. Eliceiri, NIH image to imageJ: 25 years of image analysis. *Nat. Methods* **9**, 671–675 (2012).
39. F. Norén, *Small Plastic Particles in Coastal Swedish Waters* (KIMO, Sweden, 2007).
40. V. Hidalgo-Ruz, L. Gutow, R. C. Thompson, M. Thiel, Microplastics in the marine environment: A review of the methods used for identification and quantification. *Environ. Sci. Technol.* **46**, 3060–3075 (2012).
41. M. R. Jung *et al*., Validation of ATR FT-IR to identify polymers of plastic marine debris, including those ingested by marine organisms. *Mar. Pollut. Bull.* **127**, 704–716 (2018).
42. C. Hu, X. Li, W. G. Pichel, F. E. Muller-Karger, Detection of natural oil slicks in the NW Gulf of Mexico using MODIS imagery. *Geophys. Res. Lett.* **36**, L01604 (2009).
43. S. Sun *et al*., Remote sensing assessment of oil spills near a damaged platform in the Gulf of Mexico. *Mar. Pollut. Bull.* **136**, 141–151 (2018).